WOODHEAD PUBLISHING SERIES IN CIVIL AND STRUCTURAL ENGINEERING

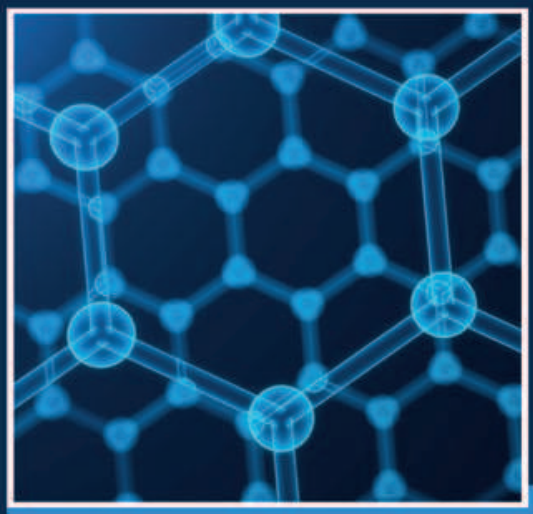

Nanotechnology in Eco-efficient Construction

Materials, Processes and Applications

Second Edition

Edited by F. Pacheco-Torgal, M. V. Diamanti, A. Nazari, C. G. Granqvist, A. Pruna, S. Amirkhanian

WP
WOODHEAD PUBLISHING

Concrete with nanomaterials and fibers for self-monitoring of strain and cracking subjected to flexure

12

Yining Ding [1], *Genjin Liu* [1], *Zhibo Han* [1], *F. Pacheco-Torgal* [2], *António Augusto Veloso de Costa* [2]
[1]Dalian University of Technology, Dalian, China; [2]University of Minho, Braga, Portugal

12.1 Introduction

Crack diagnosing is relevant for crack control in serviceability limit state and for durability requirements of concrete members. The monitoring of load-bearing capacity regarding the whole load−deflection curve can be evaluated as one of the significant points of the safety of the structure members. Real-time structural health monitoring systems may be able to assist engineers using nondestructive testing and early damage detection, so that proper maintenance can be applied. Electrically conductive concrete could be capable of sensing its own strain and damage by the electrical resistance measurement (Wen and Chung, 2006; Li et al., 2006; Wen and Chung, 2006; Chen and Liu, 2008; Wen and Chung, 2000; Azhari and Banthia, 2012; Wen and Chung, 2003; Wen and Chung, 2007; Ding et al., 2016; Ding et al., 2013; Chung, 2001). The self-sensing ability of strain and damage of electrically conductive concrete can be one of the useful methods for the nondestructive evaluation of concrete members in practice. Furthermore, electrically conductive concrete also provides wide prospect in specialist applications, such as vibration control, electromagnetic shielding, traffic monitoring, and deicing (Shi and Chung, 1999; Yehia and Tuan, 1999; Chung, 2004).

In order to obtain electrically conductive concrete, a conductive substance like nanocarbon black (NCB), carbon fiber (CF), or steel fiber (SF) can be incorporated into a cementitious matrix (Wen and Chung, 2006; Li et al., 2006; Wen and Chung, 2006; Chen and Liu, 2008; Wen and Chung, 2000; Azhari and Banthia, 2012; Wen and Chung, 2003; Wen and Chung, 2007; Ding et al., 2016; Ding et al., 2013; Chung, 2001). The addition of short CF into concrete can form some continuous conductive pathways which carry current and play a fundamental role in the electrical transport process, consequently enhancing the electrical conductivity of concrete; CF can also decrease the shrinkage cracking and improve the durability and freezing resistance, and it does not induce a large amount of water demand.

Nanotechnology in Eco-efficient Construction. https://doi.org/10.1016/B978-0-08-102641-0.00012-8

Electrically conductive fibers, such as carbon fibers and steel fibers, are effective as admixtures for improving electrical conductivity due to the formation of a continuous conducting path (Guan et al., 2002). The NCB, with its electrical conductivity, low cost, and fine filler effect, can also be used as an ideal admixture for conductive concrete (Li et al., 2006; Wen and Chung, 2007; Chung, 2001). Prior work in the combined use of NCB and CF in cement-based materials has been reported (Wen and Chung, 2007; Ding et al., 2013; Chung, 2001). The advantage of the combined use of NCB and CF is the synergistic effect, which refers to the filling (i.e., conductive filler) of the microscopic space between adjacent fibers by NCB, thereby resulting in enhancing the electrical conductivity of composites (Wu, 2005; Cai and Chung, 2006; Yang et al., 2007; Ding, 2011). Some previous studies on the self-sensing concrete are focused on the use of monophasic or diphasic conductive materials, and the relationship between the fractional change in resistance and the tension strain before concrete cracking has been suggested. The investigations on the strain and damage of microcarbon fiber and microsteel fiber reinforced cement specimens under compression and tension have been carried out (Wen and Chung, 2006; Wen and Chung, 2006; Chen and Liu, 2008; Wen and Chung, 2000; Azhari and Banthia, 2012; Wen and Chung, 2003; Wen and Chung, 2007; Ding et al., 2016; Ding et al., 2013; Chung, 2001); but, there is a shortage of using microfibers or NCB as self-sensing materials because they cannot keep the conductive path after concrete cracking. Until now, the investigations are mainly concentrated on the self-sensing of concrete damage before cracking (Wen and Chung, 2006; Li et al., 2006; Wen and Chung, 2006; Chen and Liu, 2008; Wen and Chung, 2000; Azhari and Banthia, 2012; Wen and Chung, 2003; Wen and Chung, 2007; Ding et al., 2013; Chung, 2001; Shi and Chung, 1999; Yehia and Tuan, 1999; Chung, 2004; Guan et al., 2002; Wu, 2005; Cai and Chung, 2006; Yang et al., 2007; Ding, 2011). In fact, it is important to realize that the concrete bending member works usually with cracks under service load. The concrete member may lose its serviceability by excessive cracking. The crack control is one of the key points of the serviceability, and any cracking should be limited to hairline cracks for reasons of both serviceability and durability. After all, how to self-monitor the crack opening displacement and the whole load−deflection process of concrete beam is still an open problem. This work can be considered as pioneering and tentative and it paves a new path for the self-diagnosing of the crack opening displacement (COD).

One of the innovation ideas of this work is to use macrosteel fiber in the triphasic conductive materials. There are two reasons to provide macro-SF, NCB, and CF as triphasic conductive materials:

1. Macrosteel fiber can enhance the mechanical properties before cracking and avoid the brittle failure of the concrete member during the concrete cracking and bridging of the cracks.
2. In the whole process after cracking of the concrete beam, only the macro-SF is capable to restrict the crack widening, to improve the cracking resistance and toughness, to demonstrate a stable load−deflection curve, and to maintain the conductive path of the cracked concrete matrix while the NCB and micro-CF are incapable to cross the crack surfaces (Ding et al., 2009, 2016; Deutscher Beton-Verein, 1998).

Based on the investigation of the conductive materials on the workability, compression strength, and flexural strength of concrete, lots of conductive material reinforced concrete beams were investigated experimentally, in order to study the damage and the FCR of concrete beams subjected to different loading levels. The aim of this work is to analyze the effect of NCB or CF, especially of the hybrid use of NCB and short CF as diphasic conductive materials, on the FCR of concrete beam, to study the relationships between the FCR and the strain of initial geometrical neutral axis (IGNA) of concrete beam in the precracking region. Meanwhile, the self-diagnosing ability to the cracking property and to the load−deflection behavior of the concrete beam was investigated. The relationship between FCR and the crack opening displacement (COD) of triphasic electrically conductive concrete beams under bending has been established using a tentative data return method. The results show that the relationship between the FCR and crack opening displacement of concrete beams can be well linearly fitted.

12.2 Experimental investigations

12.2.1 Materials and mixture design

In this test program (Ding et al., 2013, 2016), the base mix design of concrete beams without conductive admixtures (NCB, CF, and SF) was as follows: cement CEM I 42.5R 390 kg/m^3, fly ash 155 kg/m^3; fine aggregate 848 kg/m^3 (0−5 mm), coarse aggregate 822 kg/m^3 (5−10 mm); water 272.5 kg/m^3; water−binder ratio 0.5, and superplasticizer(SP) 7.63 kg/m^3. The base mix design of concrete without conductive materials is illustrated in Table 12.1.

The NCB content with particle size ca. 30−90 nm (Fig. 12.1(a)) was between 0.1% and 0.3% by mass of binder (0.55−1.64 kg/m^3), the density of NCB was about 0.5 g/cm^3 and the volume resistivity was 2.3 Ω cm. The carbon fiber content with diameter of 12−15 μm and a length of 6 mm (Fig. 12.1(b)) was between 0.4% and 1.2% by mass of binder (2.18−6.54 kg/m^3); the density of CF was about 1.6 g/cm^{3}and the volume resistivity of CF was between 3 and 7 mΩ m. The macrosteel fiber content with a diameter of 0.55 mm and a length of 35 mm (Fig. 12.1(c)) was between 4% and

Table 12.1 Base mixture design

Cement (kg/m^3)	Fly ash (kg/m^3)	Fine aggregate (kg/m^3)	Coarse aggregate (kg/m^3)	Water/ binder ratio	SP (kg/m^3)
390	155	848	822	0.5	1.4% of the binder

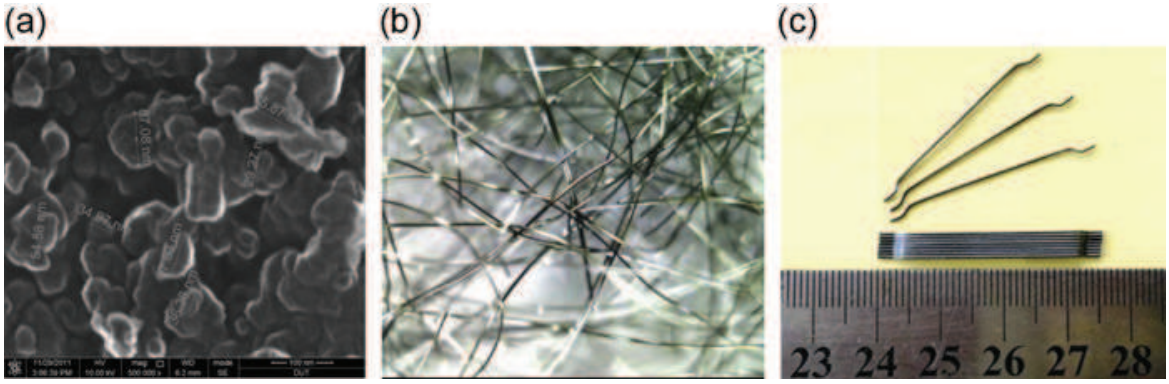

Figure 12.1 (a) Particle size of nanocarbon black using high resolution field emission SEM, (b) carbon fiber, and (c) macrosteel fiber.

8% by mass of binder (22−44 kg/m^3), the density of SF was about 7.85 g/cm^3 and the volume resistivity of SF was 10^{-6} mΩ·m. Methylcellulose was used in the amount of 0.4% by mass of cement and a defoamer was used in the amount of 0.19% of the sample volume. The different dosages of the conductive admixtures SF and BCS (NCB + CF + SF) by mass of binder in various concrete samples are compared and listed in Table 12.2.

12.2.2 Samples and set-up description

A forced mixer was used for mixing. For concrete specimens with conductive admixtures, NCB was mixed firstly with cement, fine and coarse aggregates before the addition of water, however, the carbon fiber, methylcellulose, and defoamer were dissolved or premixed with 5 L water for well dispersion of fibers. Then the premixture, NCB and superplasticizer, cement and fly ash, steel fiber and aggregate, and water were mixed for 5 min (Ding et al., 2013; Chung, 2001). The specimens prepared for testing were beams with the size of 100 mm × 100 mm × 400 mm. The specimens were demolded after 1 day and then cured at room temperature in air (relative humidity = 100%) for 28 days.

The relationships between FCR and strain, and FCR and flexural load-bearing capacity have been studied. We also analyzed the relationship between FCR and COD. The FCR measured is the fractional change in surface resistance on the tension side under bending. The dimensions and electrical contact details of all beams are shown in Fig. 12.2. For strain sensing beam four electrical contacts were prepared in the form of conductive adhesive tapes, which were adhered on the whole sides of the specimen (Fig. 12.2(a)) (Ding et al., 2013). For crack sensing specimen four electrical contacts were prepared in the form of conductive adhesive tapes, which were adhered on the tension side of the specimen (Fig. 12.2(b)) (Ding et al., 2016). Based on the four probe method of electrical resistance measurement, contacts A and D were assigned for passing current while contacts B and C were assigned for measuring the voltage (Wen and Chung, 2006).

Table 12.2 Comparison of the dosages of the conductive admixtures

Serial number		NCB mass/binder%	CF mass/binder%	SF mass/binder%
Concrete without conductive admixture	PC	0	0	0
Concrete containing NCB	NCB 01	0.1%	0	0
	NCB 02	0.2%	0	0
	NCB 03	0.3%	0	0
	NCB 04	0.4%	0	0
Concrete containing CF	CF 04	0	0.4%	0
	CF 08	0	0.8%	0
	CF 10	0	1.0%	0
	CF 13	0	1.3%	0
	CF 16	0	1.6%	0
Concrete containing BF (NCB and CF)	BF 14	0.1%	0.4%	0
	BF 18	0.1%	0.8%	0
	BF 24	0.2%	0.4%	0
	BF 28	0.2%	0.8%	0
Concrete containing SF	SF 04	0	0	4.00%
	SF 08	0	0	8.00%
Concrete containing BCS (NCB, CF, and SF)	BCS 01048	0.10% (0.55 kg/m^3)	0.40% (2.18 kg/m^3)	8.00% (44 kg/m^3)
	BCS 02084	0.20% (1.09 kg/m^3)	0.80% (4.36 kg/m^3)	4.00% (22 kg/m^3)
	BCS 01128	0.10% (0.55 kg/m^3)	1.20% (6.54 kg/m^3)	8.00% (44 kg/m^3)
	BCS 03124	0.30% (1.64 kg/m^3)	1.20% (6.54 kg/m^3)	4.00% (22 kg/m^3)

Notation: group A specimens include PC, NCB, CF, BF, and SF beams, group B specimens contain BCS beams.

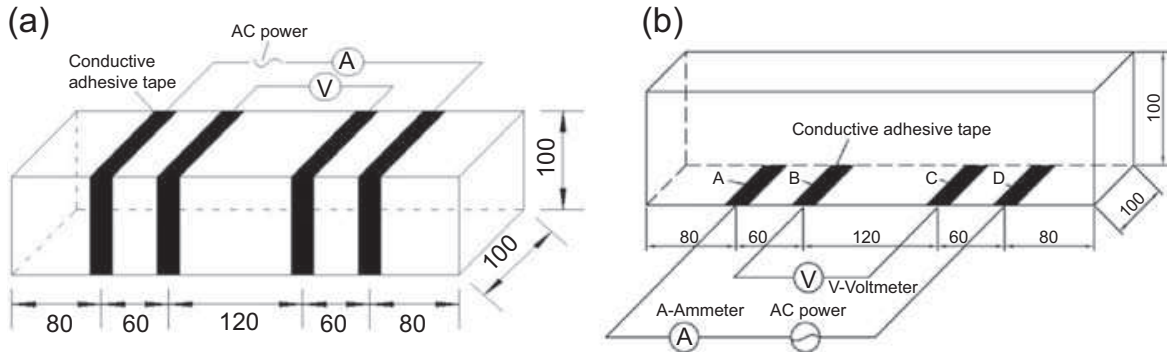

Figure 12.2 Specimen configuration for measurements of resistance of (a) strain sensing specimen and (b) crack sensing specimen.

12.2.3 Test methods

For group A specimens, the 4-pole method was adopted for the measurements of resistance. A hydraulic servo testing machine (MTS Model 810) was used. The close-loop test was controlled by displacement, and the deformation rate of net midspan was 0.2 ± 0.02 mm/min until the specified end-point deflection is reached, which was 3 kN larger than the previous loading level (Ding et al., 2016). There are two possibilities of the loading history, and the load−time relationships of the beam are illustrated in Fig. 12.3(a) and (b).

Six strain gages were applied for measuring the longitudinal strain, two of which (Strain 2(5)) were used on each side of the two opposite surfaces to measure the strain of initial geometrical neutral axis (IGNA) under the externally applied load N (Fig. 12.4.).

During the loading process, the strain near the top of concrete beam in the compression zone, the strain of IGNA, and tensile strain near the bottom of the beam have been measured by strain gages and the resistance of concrete beam has been measured simultaneously. Then the strains of IGNA can be obtained by strain gages (2) and (5). The resistance of beams was continuously measured simultaneously during

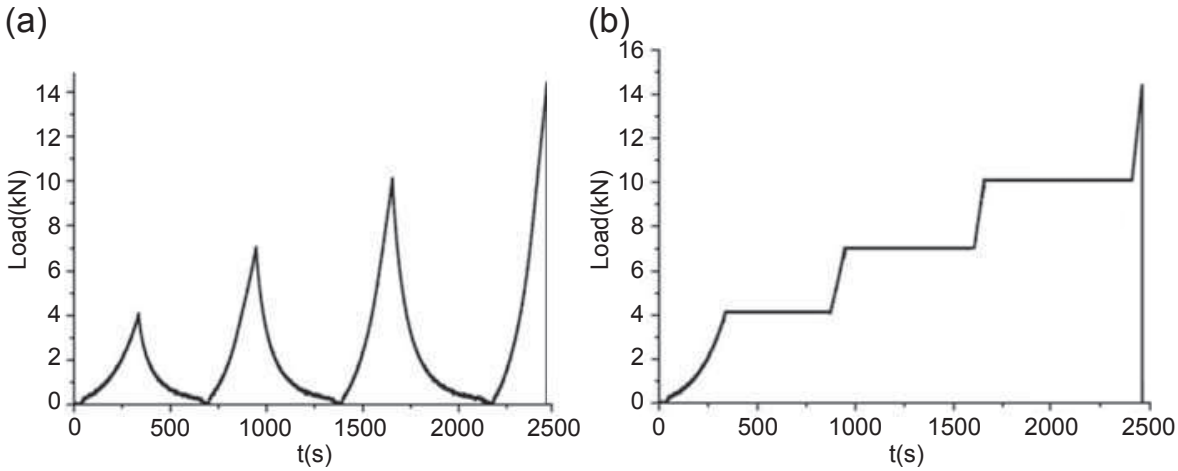

Figure 12.3 Loading histories of the beam: (a) load−time relationship I and (b) load−time relationship II.

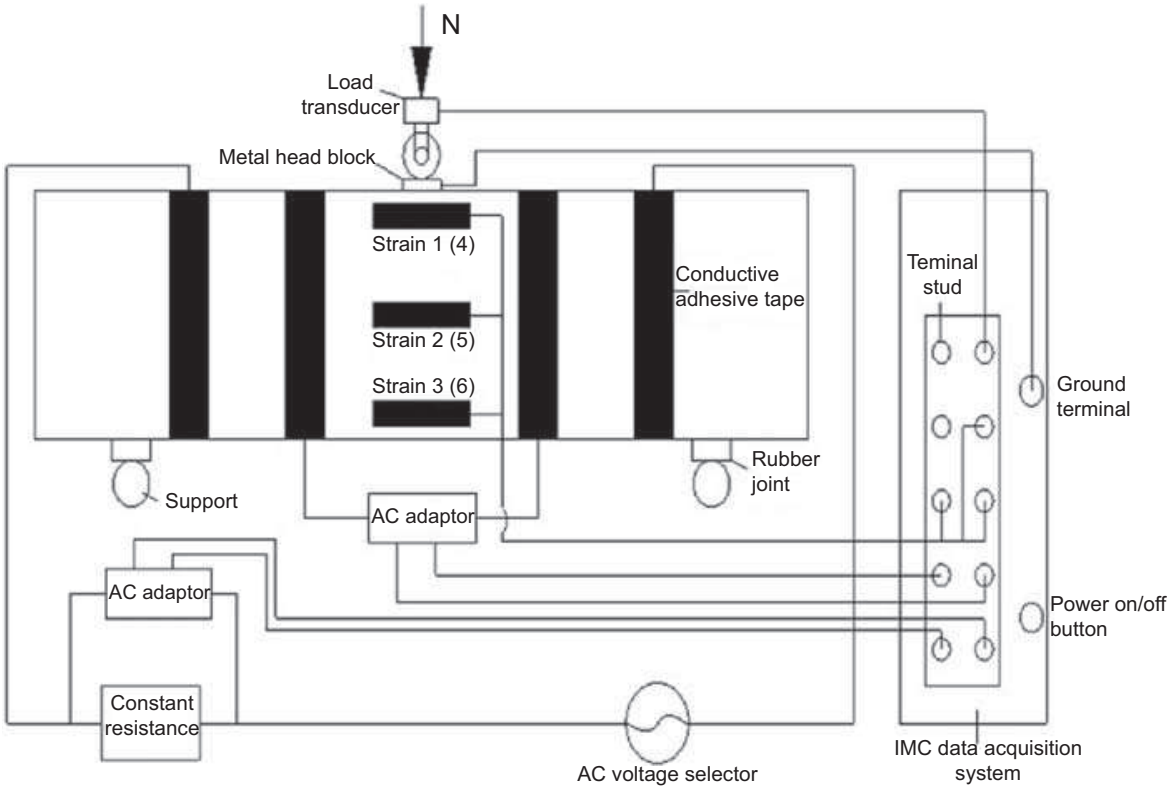

Figure 12.4 Arrangement of measuring points.

loading by using the 4-pole method previously mentioned. Other experimental instruments include an AC stabilized voltage supply, IMC Intelligence Data Collecting System, fixed resistor, and AC/DC converter. A schematic view of beam under loading with current electrodes and voltage electrodes is illustrated in Fig. 12.4. Rubber joints were used under the supporting points during the experiment (see Fig. 12.4), in order to isolate the concrete beam from the loading frame.

Group B specimens were tested under flexure over a span of 300 mm in third-point loading using a hydraulic servo testing machine (MTS 810). The close-loop test was controlled by displacement, and the deformation rate of midspan was 0.2 ± 0.02 mm/min until the specified end point deflection of 3.5 mm is reached. Two strain gages were applied at the bottom of the beam for measuring the longitudinal strain on the tension side before cracking. Two LVDTs were applied on the two

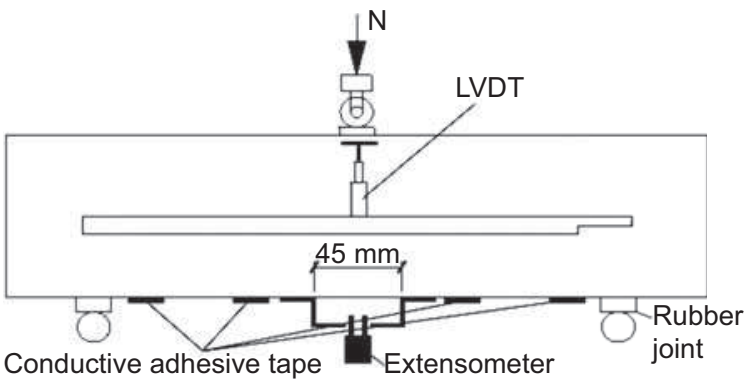

Figure 12.5 Measurement of FCR, deflection, and COD.

opposite sides for measuring deflection of midspan. An extensometer was attached at the midspan to measure the crack opening displacement during the test (see Fig. 12.5). Other experimental instruments include an AC stabilized voltage supply, IMC Intelligence Data Collecting System, fixed resistor, and AC/DC converter (Ding et al., 2016).

12.3 Influence of conductive admixtures on the mechanical and electrical properties of concrete beam

12.3.1 Influence of conductive admixtures on the workability

The workability of highly flowable fresh concrete with and without conductive admixtures has been evaluated by measuring the slump flow according to EFNARC. The experimental results of workability are listed in Table 12.3. The factor *d* represents the average diameter in the slump flow test.

From Table 12.3, it can be seen that the fresh PC (plain concrete without any conductive admixtures) corresponds well to the requirements of self-compacting concrete, and there is a very good flowability and no segregation; however, the workability

Table 12.3 Content of the conductive admixture and slump flow

Mixture/samples		Content of NCB (kg/m^3)	Content of CF (kg/m^3)	Slump flow *d* (mm)
Plain concrete	PC	0	0	620
Concrete with NCB only	NCB 01	0.3733	0	600
	NCB 02	0.7467	0	540
	NCB 03	1.1200	0	390
	NCB 04	1.4933	0	330
Concrete with CF only	CF 04	0	1.4933	590
	CF 08	0	2.9866	570
	CF 10	0	3.7333	550
	CF 13	0	4.8533	520
	CF 16	0	5.9733	500
Concrete with BF (NCB + CF)	BF 14	0.3733	1.4933	590
	BF 18	0.3733	2.9866	540
	BF 24	0.7467	1.4933	480
	BF 28	0.7467	2.9866	410

of fresh concrete declines with the increasing of NCB or CF contents. The slump flow of BF 28 is only about 410 mm. It means that the content of diphasic conductive admixtures (0.747 kg/m^3 (NCB) + 2.99 kg/m^3 (CF)) is less than the lower limit (450 mm) of the workability of highly flowable concrete. The flow behavior of NCB 03, NCB 04, and BF 28 was much less fluid than other mixtures due to the relative high content of CF and NCB.

12.3.2 Influence of conductive admixtures on the compression and flexural behavior

12.3.2.1 Effect of conductive materials on the compressive and flexural strength

The average values of the compressive strength (f_{cu}) of three specimens at the age of 28 d can be found in Table 12.4. The increment of the compression strength ranges between 1.6% and 7.5%. It means that the addition of NCB, CF, and macro-SF demonstrates some positive effect on the compressive strength of concrete, but does not show significant trend of improving compressive strength. The flexural strength and toughness parameters (the equivalent flexural strength and energy absorption capacity) of beams with different conductive admixture contents have been investigated based on German Guideline [22]. The flexural strength (σ_u) and toughness parameters are shown in Table 12.4. Fig. 12.6(a) shows the comparison of the load−deflection curves of plain concrete (PC) beam and beams with different NCB, CF, and 22 kg/m^3 SF; the comparisons of the load−deflection relationships of PC beam and beams with different NCB, CF, and 44 kg/m^3 SF are illustrated in Fig. 12.6(b). Table 12.5 shows the increase rate (δr) of the flexural strength and toughness parameters (the energy absorption and the equivalent flexural strength) with different conductive admixture contents.

Table 12.4 Comparison of the flexural and compressive strength, the equivalent flexural strength, and energy absorption of beams with different conductive admixtures

Samples	f_{cu} N/mm^2	F_u kN	σ_u N/mm^2	D^f_{BZ2} kN·mm	Equ.β_{BZ2} N/mm^2	D^f_{BZ3} kN·mm	Equ.β_{BZ3} N/mm^2
PC	35.6	13.23	4.0	–	–	–	–
SF 04	36.2	14.97	4.5	1.48	0.89	13.05	1.30
SF 08	37.8	19.46	5.8	7.49	4.49	38.13	3.81
BCS 02084	36.9	17.08	5.1	1.96	1.18	17.21	1.72
BCS 03124	37.4	18.22	5.5	2.50	1.50	18.27	1.83
BCS 01048	38.3	22.77	6.8	9.02	5.41	51.55	5.16
BCS 01128	35.9	26.29	7.9	7.48	4.49	50.04	5.00

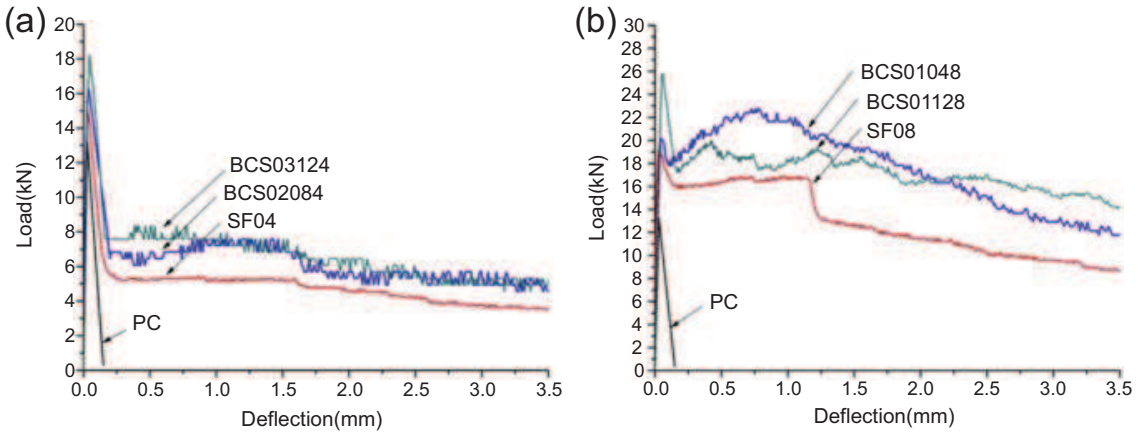

Figure 12.6 Comparison of load−deflection curves of conductive concrete beams: (a) curves of the PC beam and beams with 22 kg/m^3 SF and (b) curves of the PC beam and beams with 44 kg/m^3 SF.

It must be emphasized that there is not any toughness or postcrack energy absorption for plain concrete because the PC beam showed a strong brittle behavior and is broken down after cracking. From Table 12.4 and Fig. 12.6(a) and (b), it can be seen that:

- Compared with the plain concrete (PC) beam without any conductive admixtures (Fig. 12.6(a)), the flexural strength σ_u of SF 04 (beams with 22 kg/m^3 SF), BCS 02084 (beams with 1.1 kg/m^3 NCB, 4.36 kg/m^3 CF, and 22 kg/m^3 SF), and BCS 03124 (beams with 1.65 kg/m^3 NCB, 6.54 kg/m^3 CF, and 22 kg/m^3 SF) increased by 12.5%, 27.5%, and 37.5%, respectively.
- Compared with the PC beam (Fig. 12.6(b)), the flexural strength σ_u of SF 08 (beams with 44 kg/m^3 SF), BCS 01048 (beams with 0.55 kg/m^3 NCB, 2.18 kg/m^3 CF, and 44 kg/m^3 SF), and BCS 01128 (beams with 0.55 kg/m^3 NCB, 6.54 kg/m^3 CF, and 44 kg/m^3 SF) increased by 45%, 70%, and 97%, respectively. It means that the flexural strength can be improved clearly by the addition of conductive materials (NCB, CF, and macro-SF).
- Compared with beam SF 04 with 22 kg/m^3 SF only (Fig. 12.6(a)), the σ_u of BCS 02084 and BCS 03124 increased by 13% and 22%, respectively.

Table 12.5 Comparison of the increase rate (δ_r) of flexural strength and toughness parameter

Increase rates of strength and toughness	**σ_u (%)**	**D^f_{BZ2} (%)**	**Equ.β_{BZ2} (%)**	**D^f_{BZ3} (%)**	**Equ.β_{BZ3}**	**Total diphasic conductive materials (%)**
δ_r (BCS 02084-SF 04)	13.3	32.4	32.6	31.9	32.3	20.0
δ_r (BCS 03124-SF 04)	22.2	68.9	68.5	40.0	40.8	30.0
δ_r (BCS 01048-SF 08)	17.2	20.4	20.5	35.2	35.4	5.0
δ_r (BCS 01128-SF 08)	36.2	0.0	0.0	31.2	31.2	15.0

- Compared with beam SF 08 with 44 kg/m^3 SF only (Fig. 12.6(b)), the σ_u of BCS 01048 and BCS 01128 increased by 17% and 36%, respectively. It means that the combined use of conductive admixtures (NCB, CF, and SF) showed a positive hybrid effect on the flexural strength.
- Compared to the postcrack behavior of beams with only SF (Fig. 12.6(a) and (b)), the triphasic conductive beams behave much better over the entire deflection range. The hybrid use of NCB, CF, and macro-SF has a positive hybrid effect on the flexural toughness.

12.3.2.2 *Effects of conductive materials on the flexural toughness*

The postcrack parameters for SF 04, BCS 02084, BCS 03124, SF 08, BCS 01048, and BCS 01128 after 28 days are demonstrated in Table 12.4. Table 12.5 shows the increase rate (δ_r) of the flexural strength and toughness parameters (the energy absorption and the equivalent flexural strength) and the contents of total triphasic conductive materials.

Tables 12.4 and 12.5 show that:

1. Theplain concrete (PC) beam without conductive materials does not show any toughness. Compared with the PC beam, the addition of conductive admixtures could enhance both the flexural strength and the postcrack behavior or flexural toughness greatly.
2. Compared to SF 04 with 22 kg/m^3 SF,
   a. the toughness parameter (the energy absorption D^f_{BZ2}, D^f_{BZ3}, and the equivalent flexural strength Equ.β_{BZ2}, Equ.β_{BZ3}) of BCS 02084 increased about 32%, when the dosage of total conductive materials (NCB, CF, and SF) in BCS 02084 increased only 20%.
   b. The energy absorption D^f_{BZ2} and D^f_{BZ3}, and the equivalent flexural strength Equ.β_{BZ2} and Equ.β_{BZ3} of BCS 03124 increased 68% and 40%, respectively, when the dosage of total conductive materials in BCS 03124 increased by 30% only.
3. Compared to SF 08,
   a. the energy absorption D^f_{BZ2} and D^f_{BZ3}, and the equivalent flexural strength Equβ_{BZ2} and Equβ_{BZ3} of BCS 01048 increased 20% and 35%, respectively, although the dosage of total conductive materials (NCB, CF, and SF) in BCS 01048 increased by only 5%.
   b. Although the energy absorption D^f_{BZ2} and the equivalent flexural strength Equ.β_{BZ2} of BCS 01128 did not increase, the energy absorption D^f_{BZ3} and the equivalent flexural strength Equ.β_{BZ3} increased by 31%, when the dosage of total conductive materials in BCS 03124 increased by 15% only.

The hybrid use of nanocarbon black, carbon fiber, and macrosteel fiber has a positive hybrid effect on the flexural behavior. Comparing SF 04 with SF 08, it can be seen that the steel fiber plays a dominant role in improving the flexural behavior, especially the flexural toughness.

12.3.3 *Influence of conductive admixtures on the relationship between strain and FCR (self-monitoring of strain)*

Figs.12.7–12.10 illustrate the relationships between FCR and the strain of IGNA (ε_2) of concrete beams, and the effects of various conductive admixtures on these relationships can also be observed; it can be seen that the relationship between the FCR and the

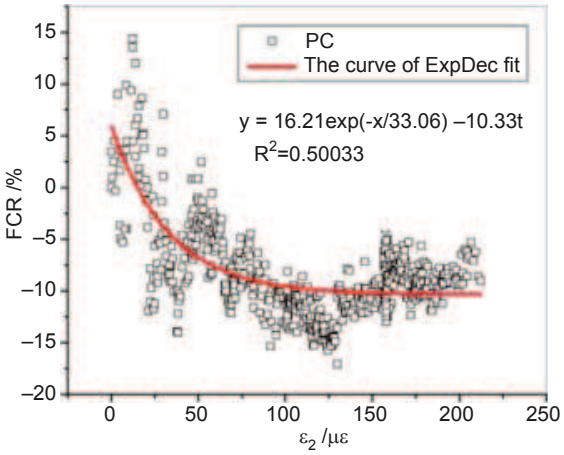

Figure 12.7 Relationship between FCR and ε2 of PC.

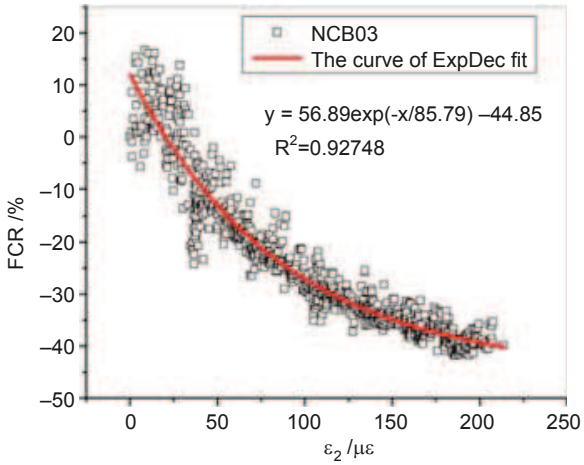

Figure 12.8 Relationship between FCR and ε2 of NCB 03.

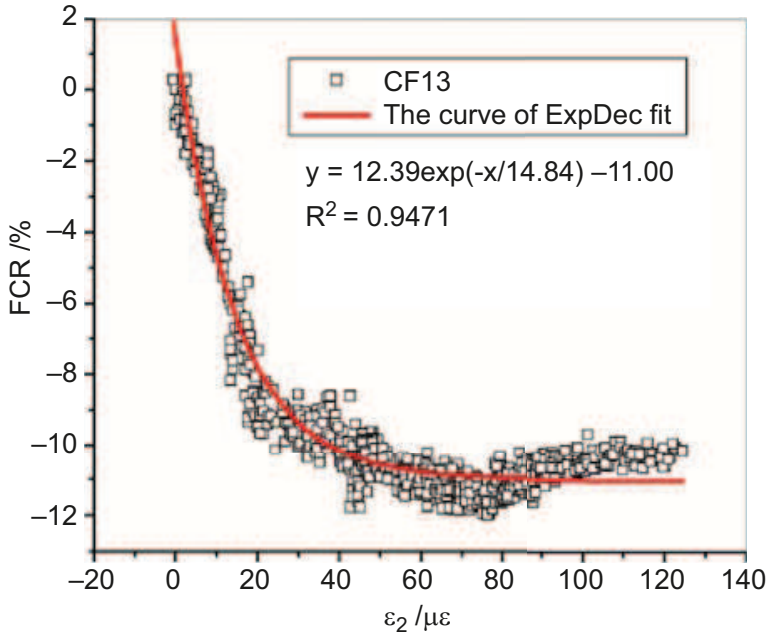

Figure 12.9 Relationship between FCR and ε2 of CF 13.

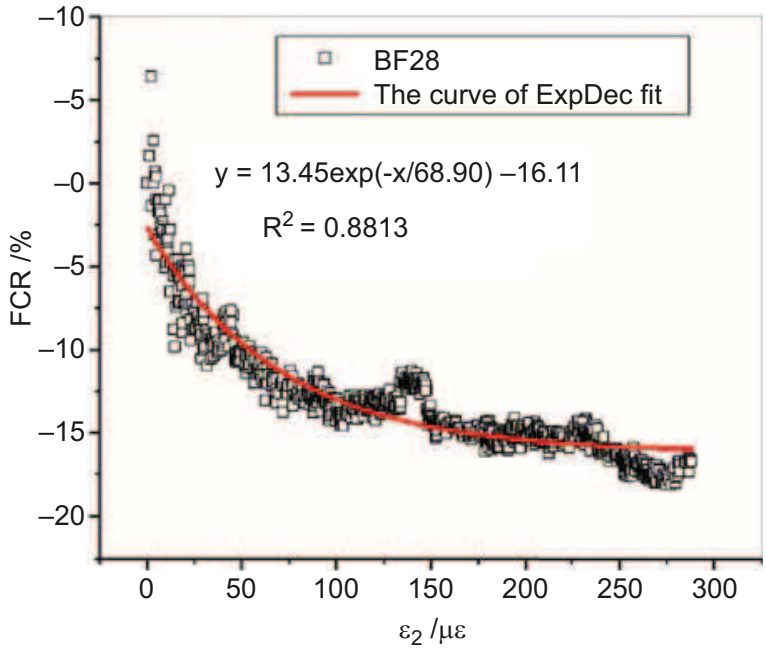

Figure 12.10 Relationship between FCR and ε2 of BF 28.

strain of IGNA corresponds well with the first order exponential decay function, which can be expressed in Eq. (12.1):

$$Y = m\exp(-X/n + p) \tag{12.1}$$

where a, b, and c are constant parameters corresponding to the type and the amount of electrical conductive phase, the variable X is the strain of IGNA, the unit of X is in με, and the FCR is the percentage of Y. The parameters fitted and the correlation coefficient C_R^2 are illustrated in Table 12.6.

The correlation coefficients of all beams in Table 12.6 range from 0.5 to 0.978. From Figs.12.7−12.10 and Table 12.6, it can be seen that:

a. The correlation coefficient C_R^2 of the plain concrete (PC) beam is only 0.50. It means that for the PC beam without conductive admixtures the tested value is not strongly related to the predicted Eq. (4).

b. The correlation coefficient C_R^2 of other beams with conductive materials like NCB, CF, or diphasic electric conductive materials (NCB + CF) is higher than 0.76. Hence, the relationship between FCR and strain of IGNA is quite strongly correlated with Eq. (4).

c. The correlation coefficient C_R^2 of NCB 03, NCB 04, CF 10, CF 13, BF 14, and B 24 is higher than 0.9. It means that the relationship between FCR and strain of IGNA is very strongly correlated with Eq. (4), and the self-diagnosing of the damage could be more suitable especially for a concrete member with the suggested contents of conductive admixtures.

d. The curves in Figs.12.7−12.10 demonstrate a monotone decreasing relationship between FCR and the strain of IGNA.

Table 12.6 Fitted parameters of regression equation

Serial number	Constant m	Constant n	Constant p	Correlation coefficient C_R^2
PC (NCB 0% + CF 0%)	16.21	33.06	−10.33	0.50033
NCB 01 (NCB 0.1% + CF 0%)	32.31	47.48	−21.05	0.82466
NCB 02 (NCB 0.2% + CF 0%)	34.57	5.21	−39.11	0.76742
NCB 03 (NCB 0.3% + CF 0%)	56.89	85.79	−44.85	0.92748
NCB 04 (NCB 0.4% + CF 0%)	23.04	17.57	−25.56	0.90907
CF 04 (NCB 0% + CF 0.4%)	27.87	13.00	−29.74	0.79566
CF 08 (NCB 0% + CF 0.8%)	20.83	19.26	−21.25	0.83359
CF 10 (NCB 0% + CF 1.0%)	25.55	12.39	−27.41	0.97752
CF 13 (NCB 0% + CF 1.3%)	12.39	14.84	−11.00	0.9471
CF 16 (NCB 0% + CF 1.6%)	42.96	15.75	−52.68	0.82598
BF 14 (NCB 0.1% + CF 0.4%)	14.88	95.04	−12.56	0.95126
BF 18 (NCB 0.1% + CF 0.8%)	106.63	83.70	−82.74	0.77459
BF 24 (NCB 0.2% + CF 0.4%)	12.98	34.94	−15.24	0.90456
BF 28 (NCB 0.2% + CF 0.8%)	13.45	68.90	−16.11	0.8813

12.3.4 Influence of conductive admixtures on the relationship between FCR and flexural load-bearing capacity

Fig. 12.11(a)−(f) illustrate the variation of the load with deflection, and of the fractional change in surface resistance (FCR) on the tension side with deflection for various conductive admixture contents under bending. Compared with SF 04/SF 08 with monofiber (see Fig. 12.11(a) and (b)), the signal to noise ratio (Wen and Chung, 2003) of the FCR−deflection curve of triphasic conductive concrete is much lower which indicates that the combined use of NCB, CF, and macro-SF demonstrates the positive hybrid effect on improving the signal-to-noise ratio of FCR (see Fig. 12.11(c)−(f)).

A significant increment of FCR can be observed (Fig. 12.11(c)−(f)) during the first concrete cracking. For instance, the FCR of BCS 01048 in Fig. 12.11(f) increased strongly during the first concrete cracking. After cracking, the FCR increased with decreasing load-bearing capacity, especially for a clear perturbation over the deflection range between 0.60 and 0.74 mm, where the load-bearing capacity dropped. A similar phenomenon can be observed for BCS 01128 (Fig. 12.11(d)) over the deflection range between 0.46 and 1.20 mm. This can reflect that the triphasic electrically conductive concrete can be very suitable for self-sensing of change of load-bearing capacity.

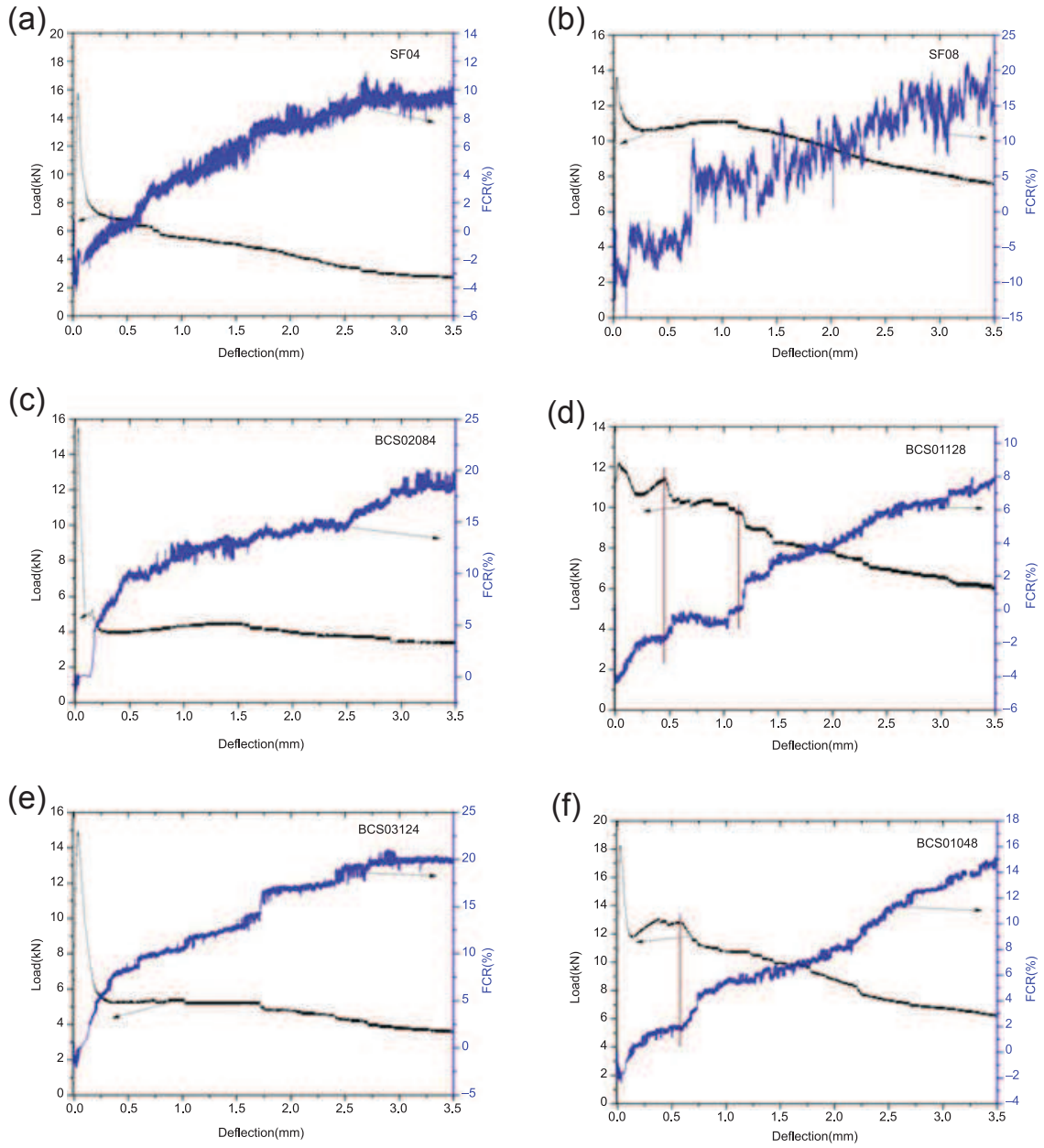

Figure 12.11 Relationships between load and deflection, FCR and deflection of (a) SF 04, (b) SF 08, (c) BCS 02084, (d) BCS 01128, (e) BCS 03124, and (f) BCS 01048.

12.3.5 *Influence of conductive admixtures on the relationship between FCR and crack opening displacement*

Figs.12.12(a)−(f) illustrate the relationship between FCR and crack opening displacement (COD) on the tension side of the beam with different conductive admixture contents under bending. They demonstrate a monotone increasing relationship between the FCR and COD, and the FCR correlates linearly with the COD.

The relationship between FCR (denoted by Y) and COD (denoted by X) can be expressed in Eq. (12.2):

$$Y = a + bX \tag{12.2}$$

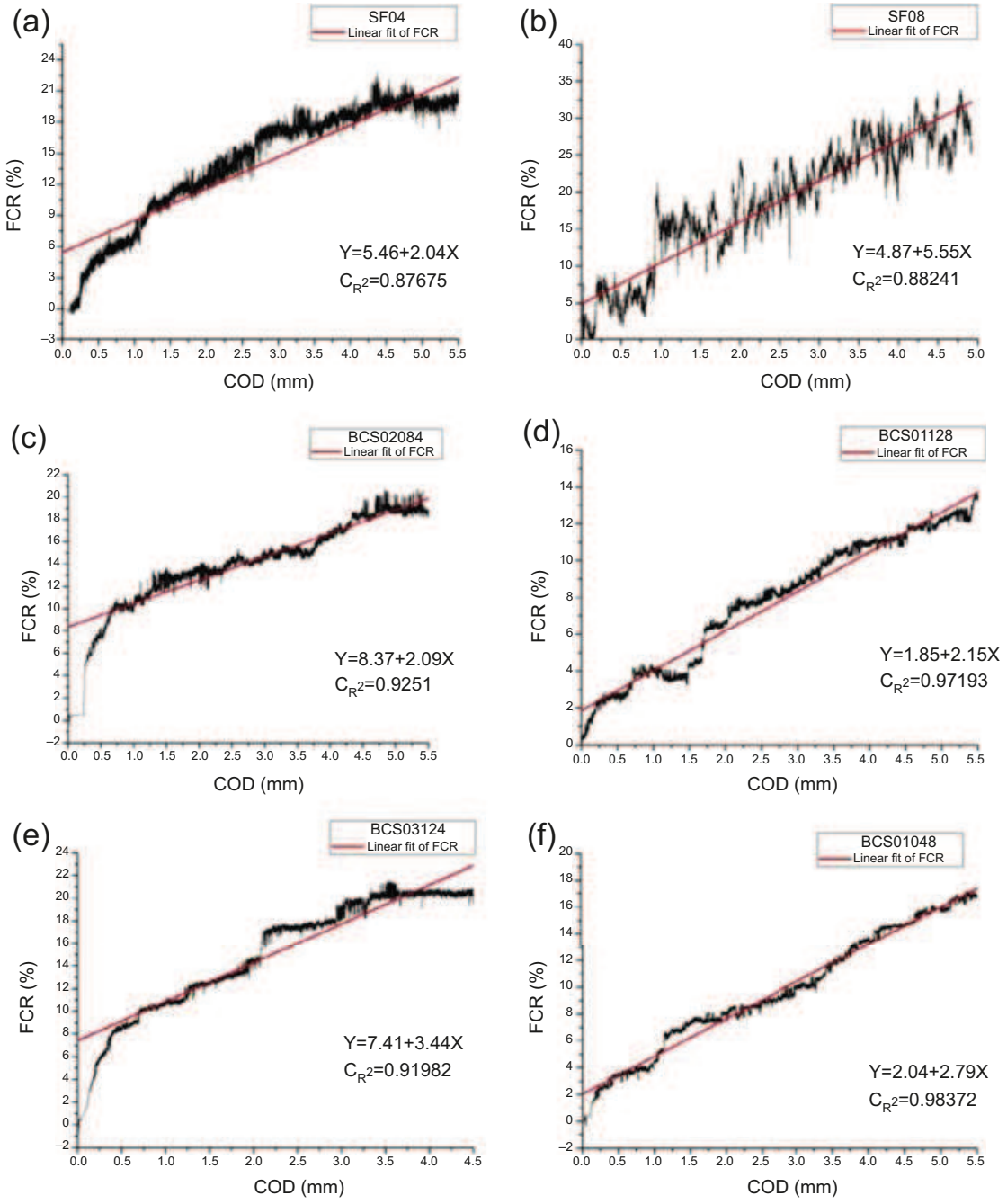

Figure 12.12 Relationships between FCR and COD of (a) SF 04, (b) SF 08, (c) BCS 02084, (d) BCS 01128, (e) BCS 03124, and (f) BCS 01048.

where *a* denotes the intercept and *b* denotes the slope of fitting line; both are constant parameters related to the types and the contents of electrically conductive phases. The unit of *X* is mm. The parameters fitted and the correlation coefficients (C_R^2) are illustrated in Table 12.7.

In addition, it can be observed from Fig. 12.11 and 12.12 that the signal-to-noise ratio of FCR (Wen and Chung, 2003) is lower than those with mono-SF. It means that the combined use of NCB, CF, and SF has a positive hybrid effect on improving the signal-to-noise ratio of FCR.

Table 12.7 Fitted parameters of regression equation

Serial number	Constant *a*	Constant *b*	Correlation coefficient C_R^2
SF 04	5.88	2.04	0.87675
SF 08	4.87	5.55	0.88241
BCS 02084	8.37	2.09	0.92510
BCS 03124	7.41	3.44	0.91982
BCS 01048	2.04	2.80	0.98372
BCS 01128	1.85	2.15	0.97193

From Table 12.7, it can be seen that:

- The correlation coefficient C_R^2 of all beams ranges from 0.88 to 0.98. It means that the relationship between the FCR and COD is very strongly correlated with Eq. (1).
- Compared with SF 04 and SF 08 (macrosteel fiber as the sole conductive admixture), the correlation coefficients C_R^2 of triphasic conductive concrete beams are higher, which means that the combined use of NCB, CF, and SF has a positive hybrid effect on C_R^2 of the concrete member.
- The parameter **b** is the slope of Eq. (1), represents the gauge factor (Wen and Chung, 2003) (the fractional change in resistance per unit COD), and can reflect the self-sensing ability to COD. The gauge factor **b** of all beams ranges from 2.04 to 5.55.
- The parameter **a** of all beams ranges from 1.85 to 8.37. Generally, the value decreases with the increase of the steel fiber content. It means that the macro-SF may work both as a structural material for enhancing the postcrack behavior of concrete and as a functional material for improving the conductivity of concrete after cracking.
- The values of *a* of BCS 02084 and BCS 03124 are larger than the others (Table 12.7), which can be attributed to the decreasing magnitude of load bearing capacity and increasing of FCR when concrete is cracking (see Fig. 12.11). Thus, the value of the intercept *a* of Eq. (1) could reflect the reducing of load-bearing capacity at cracking. The conductive concrete is suitable for the self-sensing of crack. The hybrid use of NCB, CF, and SF has a positive hybrid effect on the crack sensing ability.

12.4 Conclusion

The purpose of this study was to explore the application of the NCB, CF, and macro-SF as triphasic electrically conductive materials for self-sensing of crack of concrete beams. A series of experiments and analyses on the mechanical properties like the strength and postcrack behavior, and the electrical properties like the FCR of concrete beam with electrically conductive materials have been performed, and the effects of macro-SF and triphasic conductive materials on the relationships among the FRC, the load bearing capacity, and deflection of the concrete beam after cracking have

been evaluated. The relationship between the FCR and COD has been developed. The experimental and analytical results have led to the following conclusions:

1. The concrete conductivity increases with the increasing of the dosages of NCB and CF; however, for concrete in the practice, the workability of fresh concrete is an important precondition for selecting the types and content of the conductive materials.
2. The workability declines with the increasing of NCB or CF contents, and the upper limit of the dosage of conductive materials is determined mainly by the workability and not by the conductivity. This point was ignored in the previous investigations.
3. Compared with the plain concrete member, the addition of conductive admixtures could improve the flexural strength.
4. The macrosteel fiber plays a dominant role in improving the flexural strength and toughness.
5. As the load-bearing capacity declines rapidly at the first cracking point, the FCR of triphasic electrically conductive concrete beams shows a clear linear increase.
6. The strain of IGNA (ε_2) is a function of FCR. Before the concrete cracks, the first order exponential decay function agrees well with the relationship between ε_2 and |FCR| during the loading process of CFRC beams.
7. The FCR increases with the decreasing of the load-bearing capacity over the entire postcrack zone of the concrete beam. Triphasic electrically conductive concrete beams could reflect both the crack opening displacement and the decreasing of load-bearing capacity under bending.
8. The FCR correlates linearly well with the crack opening displacement on the tension side of the conductive concrete beam.
9. Compared with the concrete beam with only steel fiber, the hybrid use of NCB, CF, and macro-SF shows a clear positive hybrid effect on the flexural behavior and self-sensing ability to crack widening.

References

Azhari, F., Banthia, N., 2012. Cement-based sensors with carbon fibers and carbon nanotubes for piezoresistive sensing. Cement and Concrete Composites 34, 866−873.

Cai, S.W., Chung, D.D.L., 2006. Spatially resolved self-sensing of strain and damage in carbon fiber cement. Journal of Materials Science 41, 4823−4831.

Chen, B., Liu, J., 2008. Damage in carbon fiber-reinforced concrete, monitored by both electrical resistance measurement and acoustic emission analysis. Construction and Building Materials 22, 2196−2201.

Chung, D.D.L., 2001. Electromagnetic interference shielding effectiveness of carbon materials. Carbon 39 (2), 279−285.

Chung, D.D.L., 2004. Electrically conductive cement-based materials. Advances in Cement Research 16 (4), 167−176.

Deutscher Beton-Verein, E.V., 1998. DBV-Merkblatt, Bemessungsgrundlagen fuer Stahlfaserbeton im Tunnelbau. Eigenverlag, Wiesbaden.

Ding, Y., Zhang, Y., Thomas, A., 2009. The investigation on strength and flexural toughness of fibre cocktail reinforced self-compacting high performance concrete. Construction and Building Materials 23, 448−452.

Ding, Y., Chen, Z., Han, Z., Zhang, Y., Pacheco-Torgal, F., 2013. Nano carbon black and carbon fiber as conductive materials for the diagnosing of the damage of concrete beam. Construction and Building Materials 43, 233−241.

Ding, Y., Han, Z., Zhang, Y., et al., 2016. Concrete with triphasic conductive materials for self-monitoring of cracking development subjected to flexure. Composite Structures 138, 184−191.

Ding, Y., 2011. Investigations into the relationship between deflection and crack mouth opening displacement of SFRC beam. Construction and Building Materials 25, 2432−2440.

Guan, X.C., Han, B.G., Ou, J.P., 2002. Study on the dispersibility of carbon fiber in cement paste. China Concrete Cement Products 2, 34−36.

Li, H., Xiao, H., Ou, J., 2006. Effect of compressive strain on electrical resistivity of carbon black-filled cement-based composites. Cement and Concrete Composites 28, 824−828.

Shi, Z., Chung, D.D.L., 1999. Carbon fiber reinforced concrete for traffic monitoring and weighing in motion. Cement and Concrete Research 29, 435−439.

Wen, S., Chung, D.D.L., 2000. Uniaxial tension in carbon fiber reinforced cement, sensed by electrical resistivity measurement in longitudinal and transverse directions. Cement and Concrete Research 30, 1289−1294.

Wen, S., Chung, D.D.L., 2003. A comparative study of steel- and carbon-fiber cement as pirzoresistive strain sensors. Advances in Cement Research 15 (3), 119−128.

Wen, S., Chung, D.D.L., 2006a. Self-sensing of flexural damage and strain in carbon fiber reinforced cement and effect of embedded steel reinforcing bars. Carbon 44, 1496−1502.

Wen, S., Chung, D.D.L., 2006b. Effects of strain and damage on the strain sensing ability of carbon fiber cement. Journal of Materials in Civil Engineering 18, 355−360.

Wen, S., Chung, D.D.L., 2007. Partial replacement of carbon fiber by carbon black in multifunctional cement−matrix composites. Carbon 45, 505−513.

Wu, X., 2005. Study on relations among electric conductivity, stress and strain under the whole loading process for conductible Concrete. Journal of Management and Construction of Civil Engineering 2008 (3), 135−139.

Yang, C.Q., Wu, Z.S., Huang, H., 2007. Electrical properties of different types of carbon fiber reinforced plastics (CFRPs) and hybrid CFRPs. Carbon 45 (15), 3027−3035.

Yehia, S., Tuan, C.Y., 1999. Conductive concrete overlay for bridge deck deicing. ACI Material Journal 96 (3), 382−390.